SUPPORTING INFORMATION

Rapid Synthesis of Cerium-UiO-66 MOF Nanoparticles for Photocatalytic Dye Degradation

Ehsan Ezzatpour Ghadim[a], Marc Walker[b] and Richard I. Walton[a]*

[a]Department of Chemistry, University of Warwick, Coventry, CV4 7AL, UK

[b]Department of Physics, University of Warwick, Coventry CV4 7AL, UK

* Author for correspondence: r.i.walton@warwick.ac.uk

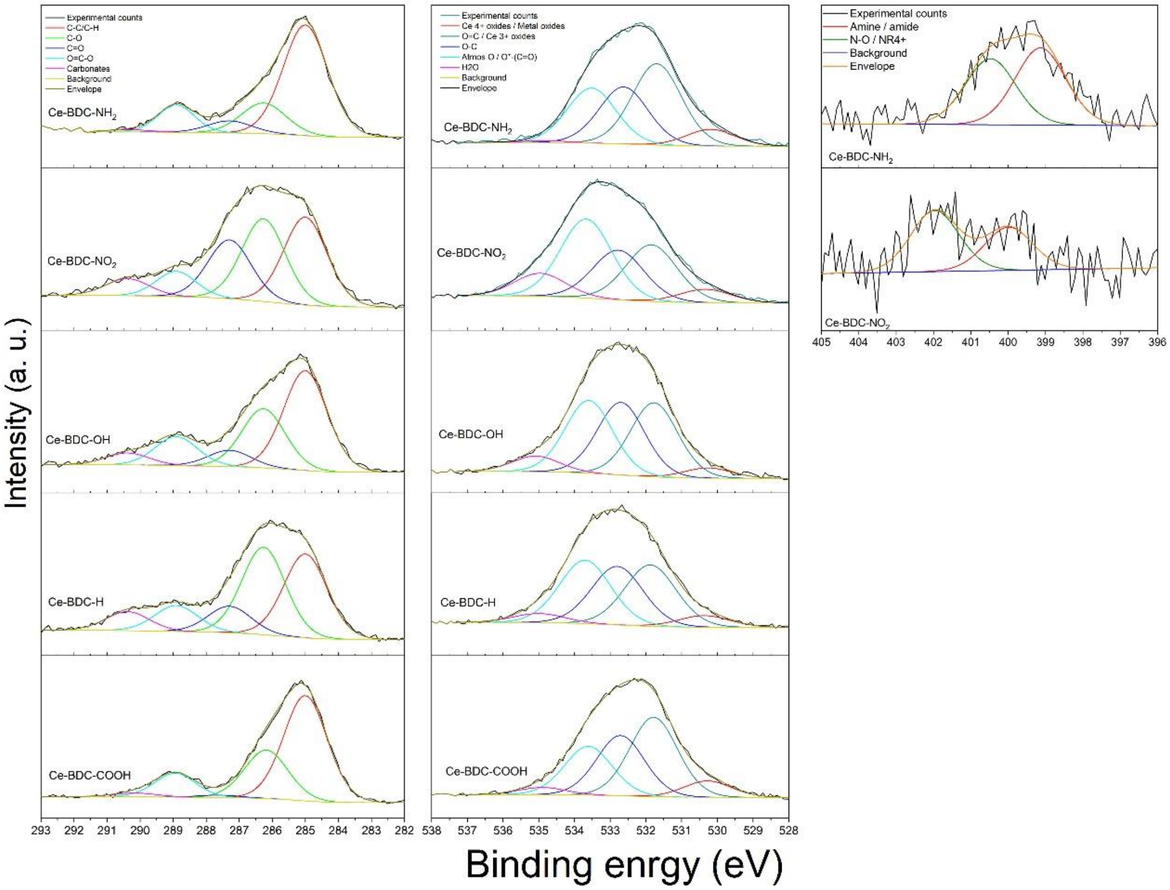

Figure S1: O 1S, C 1S, N 1S regions of the XPS spectra of the Ce-UiO-66-X series (X=NH$_2$, OH, H, NO$_2$, COOH).

Table S1a: Details of the deconvolution of XPS spectra of Ce-BDC-NH_2.

Ce 3d region			**C 1s region**			**O 1s region**		
Binding energy (eV)	*% of region*	*Bonding environment*	*Binding energy (eV)*	*% of region*	*Bonding environment*	*Binding energy (eV)*	*% of region*	*Bonding environment*
882.42	7.5	Ce 3d$_{5/2}$ - Ce^{3+}	285	62.1	C-C/C-H	530.18	7.9	Ce^{4+} oxides/metal oxides
886.36	24.2	Ce 3d$_{5/2}$ - Ce$_{3+}$	286.27	17.2	C-O / C-N	531.69	38.4	O=C /Ce^{3+} oxides
893.18	2.1	Ce 3d$_{5/2}$ - Ce^{3+}	287.29	6.8	C=O	532.62	26.9	O-C
901.21	7.4	Ce 3d$_{3/2}$ - Ce^{3+}	288.91	12.6	O=C-O	533.52	26	Atmos O / O*-(C=O)
905.15	25.8	Ce 3d$_{3/2}$ - Ce^{3+}	290.38	1.3	carbonates	534.81	0.8	H_2O
910.52	2.1	Ce 3d$_{3/2}$ - Ce^{3+}						Ce^{4+} oxides / Metal oxides
884.2	4.7	Ce 3d$_{5/2}$ - Ce^{4+}						
889.91	4.6	Ce 3d$_{5/2}$ - Ce^{4+}						
899.22	6.2	Ce 3d$_{5/2}$ - Ce^{4+}						
902.54	4.7	Ce 3d$_{3/2}$ - Ce^{4+}						
908.73	4.4	Ce 3d$_{3/2}$ - Ce^{4+}						
917.63	6.3	Ce 3d$_{3/2}$ - Ce^{4+}						

Table S1b: Details of the deconvolution of XPS spectra of Ce-BDC-OH.

Ce 3d region			**C 1s region**			**O 1s region**		
Binding energy (eV)	*% of region*	*Bonding environment*	*Binding energy (eV)*	*% of region*	*Bonding environment*	*Binding energy (eV)*	*% of region*	*Bonding environment*
883.1	8	Ce 3$d_{5/2}$ - Ce^{3+}	285	46.2	C-C/C-H	530.26	4.2	$^{Ce4+}$ oxides / Metal oxides
887.04	26.1	Ce 3$d_{5/2}$ - Ce^{3+}	286.27	27.4	C-O / C-N	531.77	30.2	O=C/Ce^{3+} oxides
893.87	2.3	Ce 3$d_{5/2}$ - Ce^{3+}	287.29	7.6	C=O	532.7	29.6	O-C
901.9	8	Ce 3$d_{3/2}$ - Ce^{3+}	288.91	13.2	O=C-O	533.6	29.6	Atmos O / O*-(C=O)
905.84	27.8	Ce 3$d_{3/2}$ - Ce^{3}+	290.38	5.6	Carbonates	535.09	6.4	H_2O
905.84	27.8	Ce 3$d_{3/2}$ - Ce^{3+}						
911.21	2.3	Ce 3$d_{3/2}$ - Ce^{3+}						
884.88	3.9	Ce 3$d_{5/2}$ - Ce^{4+}						
890.6	3.8	Ce 3$d_{5/2}$ - Ce^{4+}						
899.91	5.1	Ce 3$d_{5/2}$ - Ce^{4+}						
903.23	3.9	Ce 3$d_{3/2}$ -Ce^{4+}						
909.41	3.6	Ce 3$d_{3/2}$ - Ce^{4+}						
918.31	5.2	Ce 3$d_{3/2}$ - Ce^{4+}						

Table S1c: Details of the deconvolution of XPS spectra of Ce-BDC-H

Ce 3d region			**C 1s region**			**O 1s region**		
Binding energy (eV)	*% of region*	*Bonding environment*	*Binding energy (eV)*	*% of region*	*Bonding environment*	*Binding energy (eV)*	*% of region*	*Bonding environment*
883.21	7.9	Ce $3d_{5/2}$ - Ce^{3+}	285	34.5	C-C/C-H	530.36	5.7	Ce^{4+} oxides / Metal oxides
887.15	25.5	Ce $3d_{5/2}$ - Ce^{3+}	286.27	36	C-O / C-N	531.87	30.1	O=C / Ce^{3+} oxides
893.98	2.2	Ce $3d_{5/2}$ - Ce^{3+}	287.29	10.9	C=O	532.8	28.7	O-C
902	7.8	Ce $3d_{3/2}$ - Ce^{3+}	288.91	10.7	O=C-O	533.7	31.1	Atmos O / O*-(C=O)
905.94	27.2	Ce $3d_{3/2}$ - Ce^{3+}	290.38	7.9	Carbonates	534.99	4.5	H_2O
911.32	2.2	Ce $3d_{3/2}$ - Ce^{3+}						
884.99	4.2	Ce $3d_{5/2}$ - Ce^{4+}						
890.7	4	Ce $3d_{5/2}$ - Ce^{4+}						
900.01	5.5	Ce $3d_{5/2}$ - Ce^{4+}						
903.33	4.1	Ce $3d_{3/2}$ - Ce^{4+}						
909.52	3.9	Ce $3d_{3/2}$ - Ce^{4+}						
918.42	5.6	Ce $3d_{3/2}$ - Ce^{4+}						

Table S1d: Details of the deconvolution of XPS spectra of Ce-BDC-NO_2

Ce 3d region			**C 1s region**			**O 1s region**		
Binding energy (eV)	*% of region*	*Bonding environment*	*Binding energy (eV)*	*% of region*	*Bonding environment*	*Binding energy (eV)*	*% of region*	*Bonding environment*
883.25	6.2	Ce $3d_{5/2}$ - Ce^{3+}	285	32.6	C-C/C-H	530.33	6	Ce^{4+} oxides / Metal oxides
887.19	20	Ce $3d_{5/2}$ - Ce^{3+}	286.27	30.7	C-O / C-N	531.84	25.5	O=C / Ce^{3+} oxides
894.02	1.8	Ce $3d_{5/2}$ - Ce^{3+}	287.29	21.8	C=O	532.77	22.4	O-C
902.05	6.1	Ce $3d_{3/2}$ - Ce^{3+}	288.91	8.6	O=C-O	533.67	35.6	Atmos O / O*-(C=O)
905.99	21.3	Ce $3d_{3/2}$ - Ce^{3+}	290.38	6.4	Carbonates	534.96	10.4	H_2O
911.36	1.8	Ce $3d_{3/2}$ - Ce^{3+}						
885.03	6.6	Ce $3d_{5/2}$ - Ce^{4+}						
890.75	6.4	Ce $3d_{5/2}$ - Ce^{4+}						
900.23	8.6	Ce $3d_{5/2}$ - Ce^{4+}						
903.37	6.5	Ce $3d_{3/2}$ - Ce^{4+}						
909.56	6.1	Ce $3d_{3/2}$ - Ce^{4+}						
918.46	8.8	Ce $3d_{3/2}$ - Ce^{4+}						

Table S1e: Details of the deconvolution of XPS spectra of Ce-BDC-COOH

Ce 3d region			**C 1s region**			**O 1s region**		
Binding energy (eV)	*% of region*	*Bonding environment*	*Binding energy (eV)*	*% of region*	*Bonding environment*	*Binding energy (eV)*	*% of region*	*Bonding environment*
883.25	6.8	Ce $3d_{5/2}$ - Ce^{3+}	285	33.2	C-C/C-H	530.34	4.9	Ce^{4+} oxides / Metal oxides
887.19	22.1	Ce $3d_{5/2}$ - Ce^{3+}	286.16	40.2	C-O / C-N	531.85	23.7	O=C / Ce^{3+} oxides
894.02	1.9	Ce $3d_{5/2}$ - Ce^{3+}	287.29	12.6	C=O	532.77	27	O-C
902.05	6.8	Ce $3d_{3/2}$ - Ce^{3+}	289.01	8.5	O=C-O	533.67	37.3	Atmos O / O*-(C=O)
905.99	23.6	Ce $3d_{3/2}$ - Ce^{3+}	290.26	5.6	Carbonates	534.97	7.1	H_2O
911.36	1.9	Ce $3d_{3/2}$ - Ce^{4+}						
885.04	5.6	Ce $3d_{3/2}$ - Ce^{4+}						
890.75	5.4	Ce $3d_{3/2}$ - Ce^{4+}						
900.06	7.4	Ce $3d_{5/2}$ - Ce^{4+}						
903.38	5.6	Ce $3d_{3/2}$ - Ce^{4+}						
909.57	5.2	Ce $3d_{3/2}$ - Ce^{4+}						
918.47	7.6	Ce $3d_{3/2}$ - Ce^{4+}						

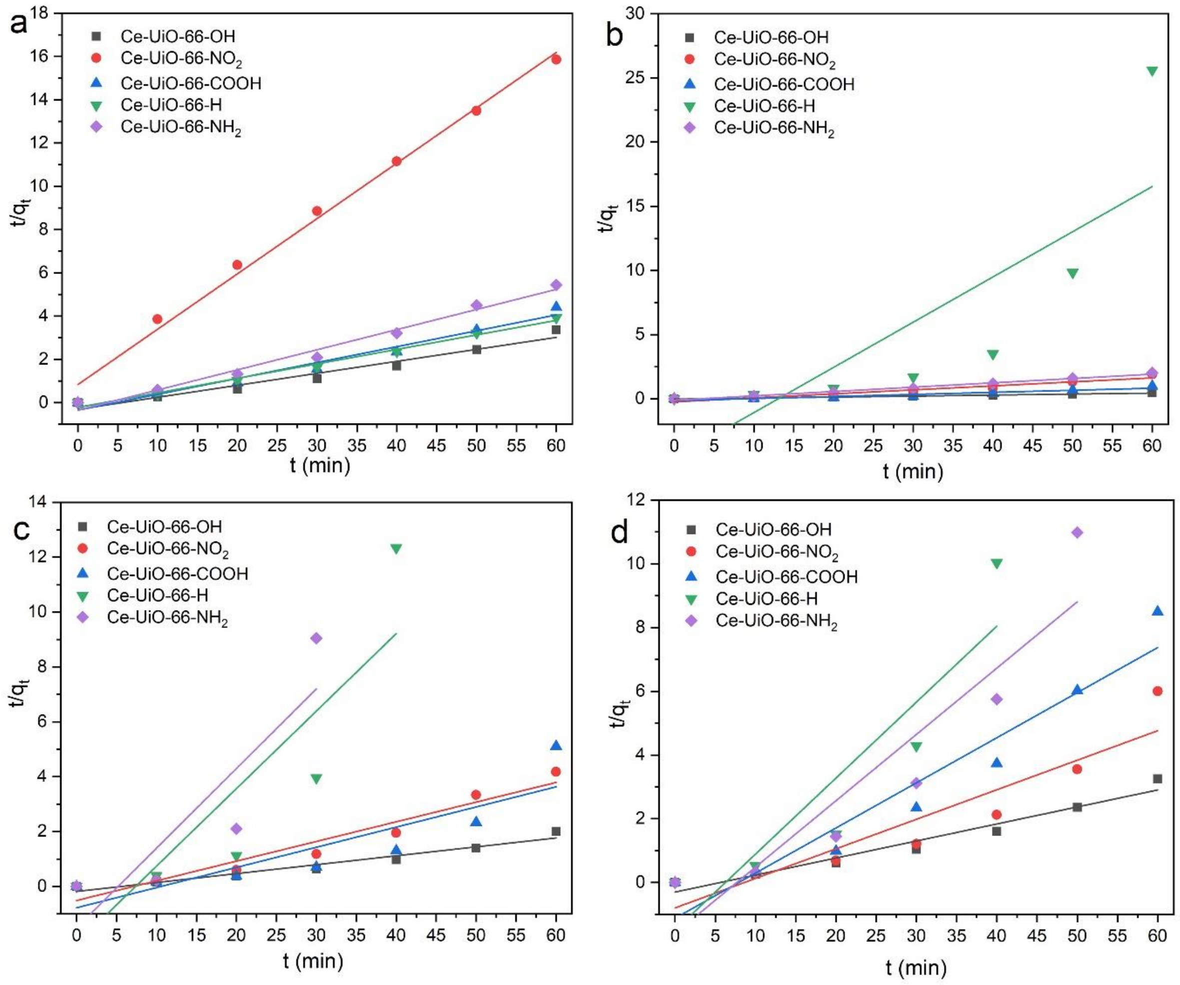

Figure S2: Pseudo-second order kinetic fits for adsorption by UiO-66-X(OH. NO_2, COOH, H, NH_2), a)MB, b)RhB, c) CR, d) AR.

Table S2: Kinetic parameters of adsorption of cationic and anionic dyes by Ce-UiO-66-X.

		Pseudo-first order			Pseudo-second order		
MOFs	Dye	k_1 (min^{-1})	q_e (mg.g^{-1})	R^2	k_2 (g·mg^{-1}min^{-1})	q_e (mg.g^{-1})	R^2
Ce-UiO-66-OH	MB	4.4×10^{-2}	50.46	0.996	1.1×10^{-2}	18.05	0.960
Ce-UiO-66-NO_2	MB	7.5×10^{-2}	60.78	0.994	7.7×10^{-2}	3.92	0.992
Ce-UiO-66-COOH	MB	4.0×10^{-2}	16.66	0.997	1.6×10^{-2}	14.28	0.980
Ce-UiO-66-H	MB	4.7×10^{-2}	16.43	0.996	2.1×10^{-4}	149.25	0.994
Ce-UiO-66-NH_2	MB	5.6×10^{-2}	9.50	0.999	2.5×10^{-2}	10.75	0.984
Ce-UiO-66-OH	RhB	5.4×10^{-2}	36.79	0.988	7.9×10^{-3}	126.58	0.993
Ce-UiO-66-NO_2	RhB	4.3×10^{-2}	97.07	0.981	1.8×10^{-3}	61.72	0.896
Ce-UiO-66-COOH	RhB	5.3×10^{-2}	42.95	0.995	4.0×10^{-2}	32.5	0.922
Ce-UiO-66-H	RhB	5.6×10^{-2}	91.26	0.996	6.7×10^{-2}	3.82	0.774
Ce-UiO-66-NH_2	RhB	3.3×10^{-2}	38.64	0.991	1.0×10^{-2}	29.49	0.985
Ce-UiO-66-OH	CR	6.6×10^{-2}	82.65	0.996	6.7×10^{-2}	28.75	0.951
Ce-UiO-66-NO_2	CR	1.4×10^{-2}	68.58	0.998	8.0×10^{-3}	12.74	0.934
Ce-UiO-66-COOH	CR	3.2×10^{-2}	98.80	0.995	6.9×10^{-3}	13.60	0.770
Ce-UiO-66-H	CR	8.0×10^{-2}	77.44	0.999	3.0×10^{-2}	7.93	0.828
Ce-UiO-66-NH_2	CR	4.6×10^{-2}	146.58	0.997	7.0×10^{-2}	3.324	0.780
Ce-UiO-66-OH	AR	5.7×10^{-2}	54.37	0.995	9.5×10^{-3}	18.72	0.957
Ce-UiO-66-NO_2	AR	4.5×10^{-2}	54.13	0.992	1.0×10^{-2}	10.78	0.868
Ce-UiO-66-COOH	AR	2.6×10^{-2}	73.75	0.977	4.2×10^{-3}	6.64	0.862
Ce-UiO-66-H	AR	3.7×10^{-2}	99.59	0.999	4.6×10^{-2}	4.47	0.834
Ce-UiO-66-NH_2	AR	4.2×10^{-2}	74.16	0.996	3.7×10^{-2}	4.79	0.865

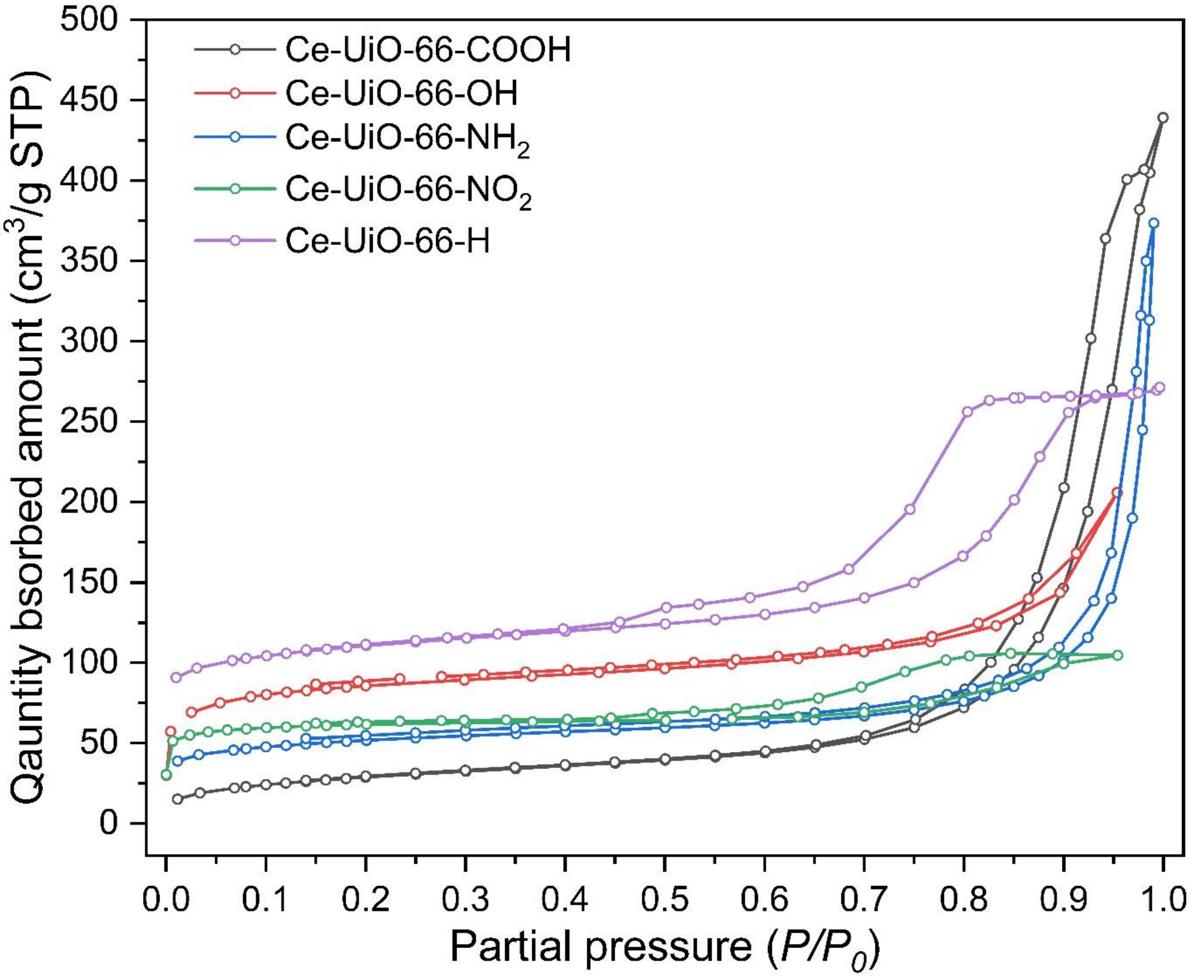

Figure S3: Nitrogen adsorption–desorption isotherms of Ce-UiO-66-X (X=COOH, OH, NH_2, NO_2, H).

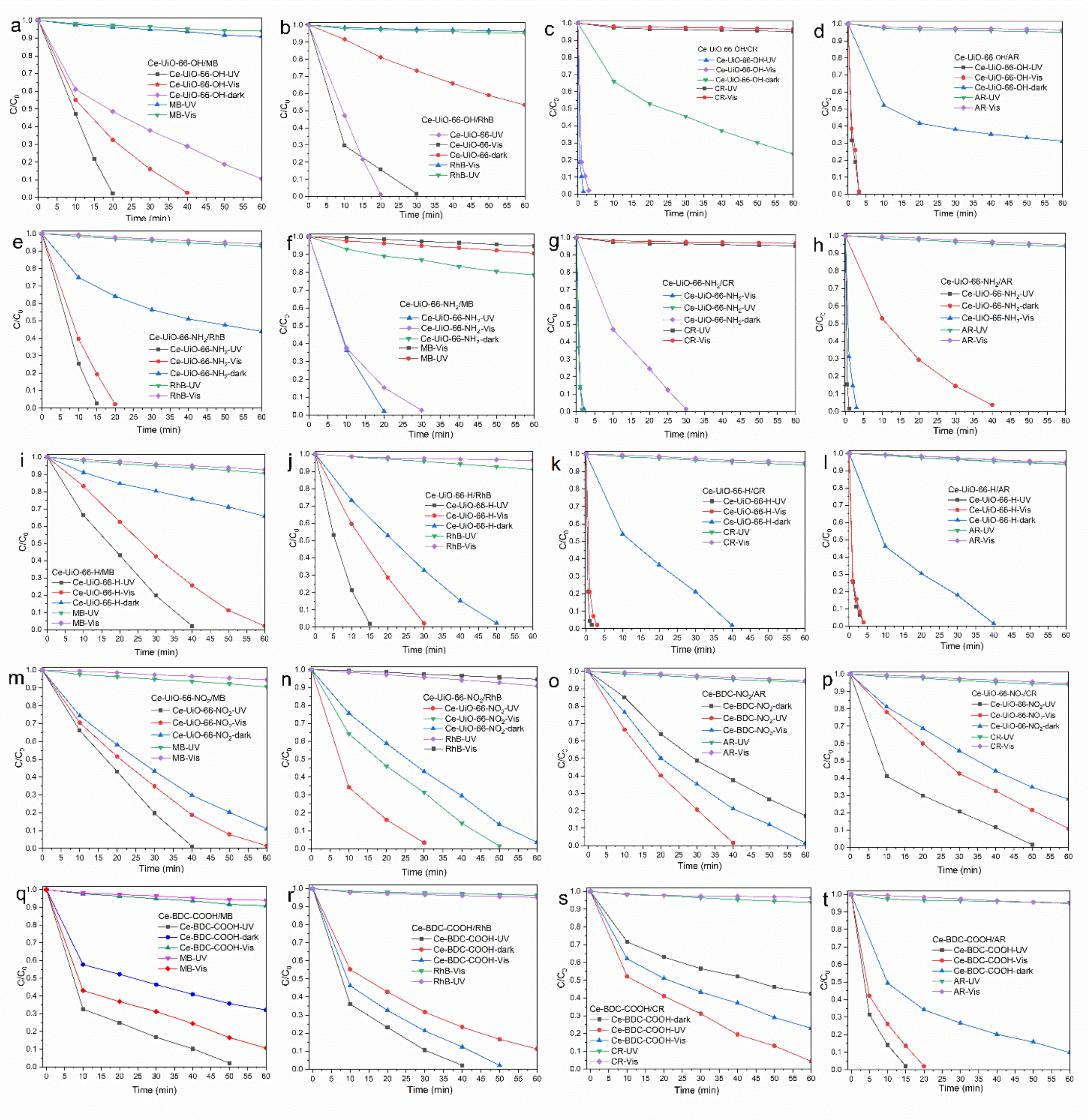

Figure S4a-t: Photocatalytic activities of Ce-UiO-66-X (NH₂, OH, H, NO₂, COOH) measured in UV, visible, and dark by two cationic (MB, RhB) and two anionic dyes (CR, AR) in 60 min.

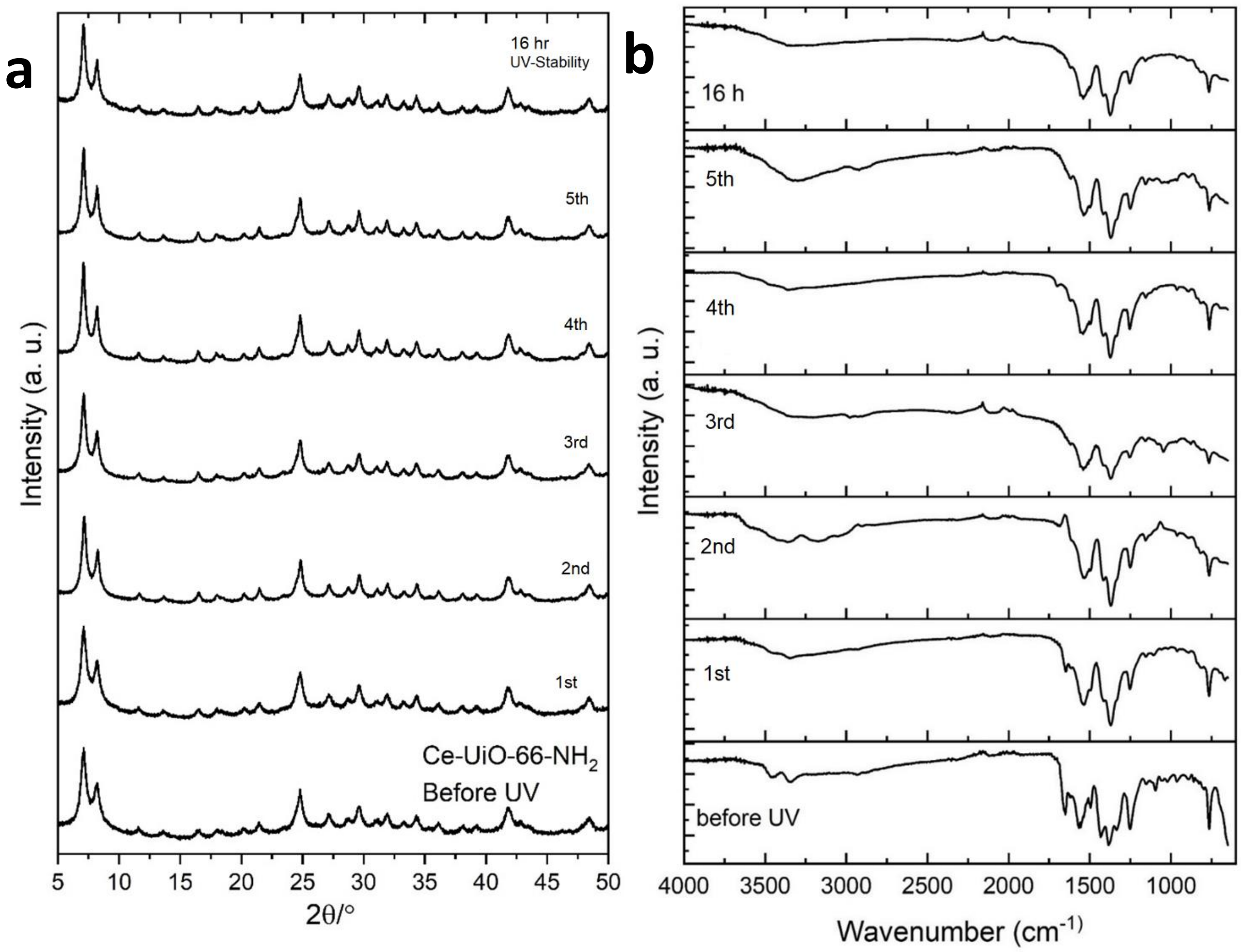

Figure S5: Recyclability after 5 cycles and 16 hours UV photostability of Ce-UiO-66-NH$_2$ a) PXRD, b) FT-IR.

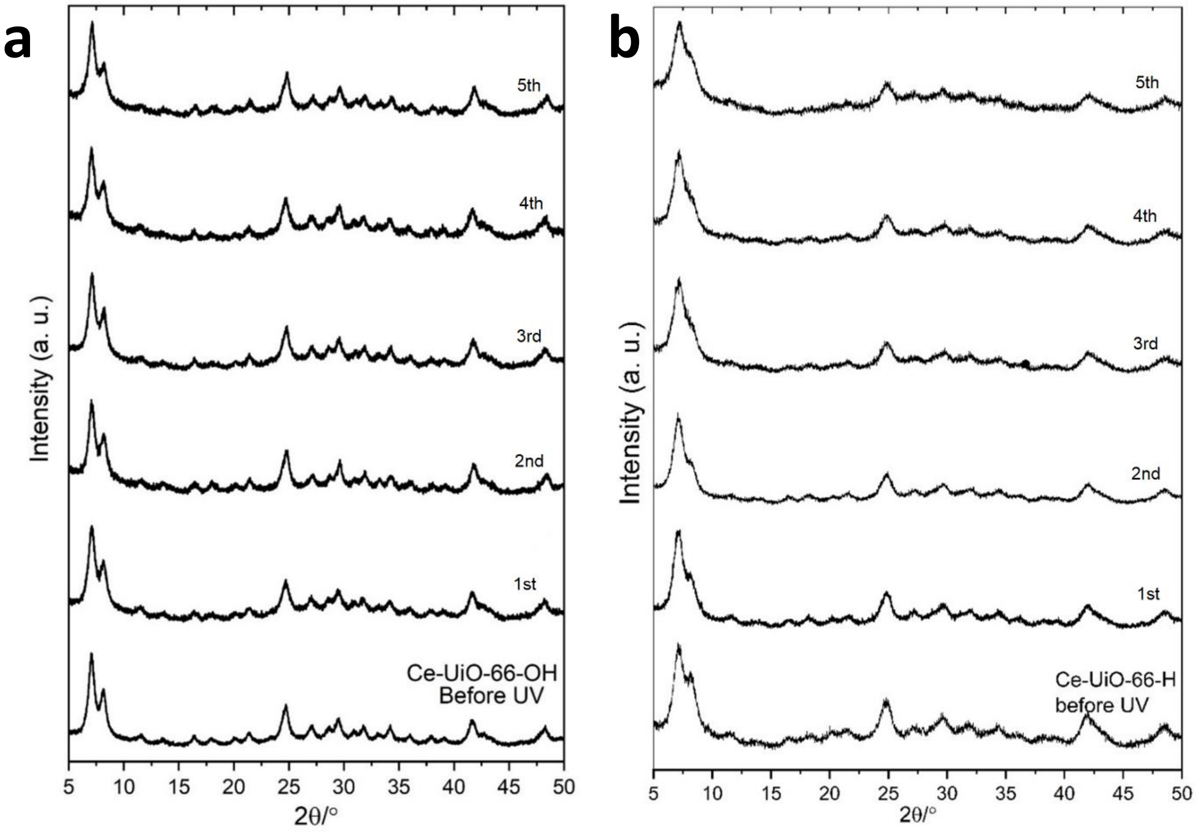

Figure S6: PXRD patterns showing recyclability after 5th cycles under light irradiation a) Ce-UiO-66-OH, b) Ce-UiO-66-H.

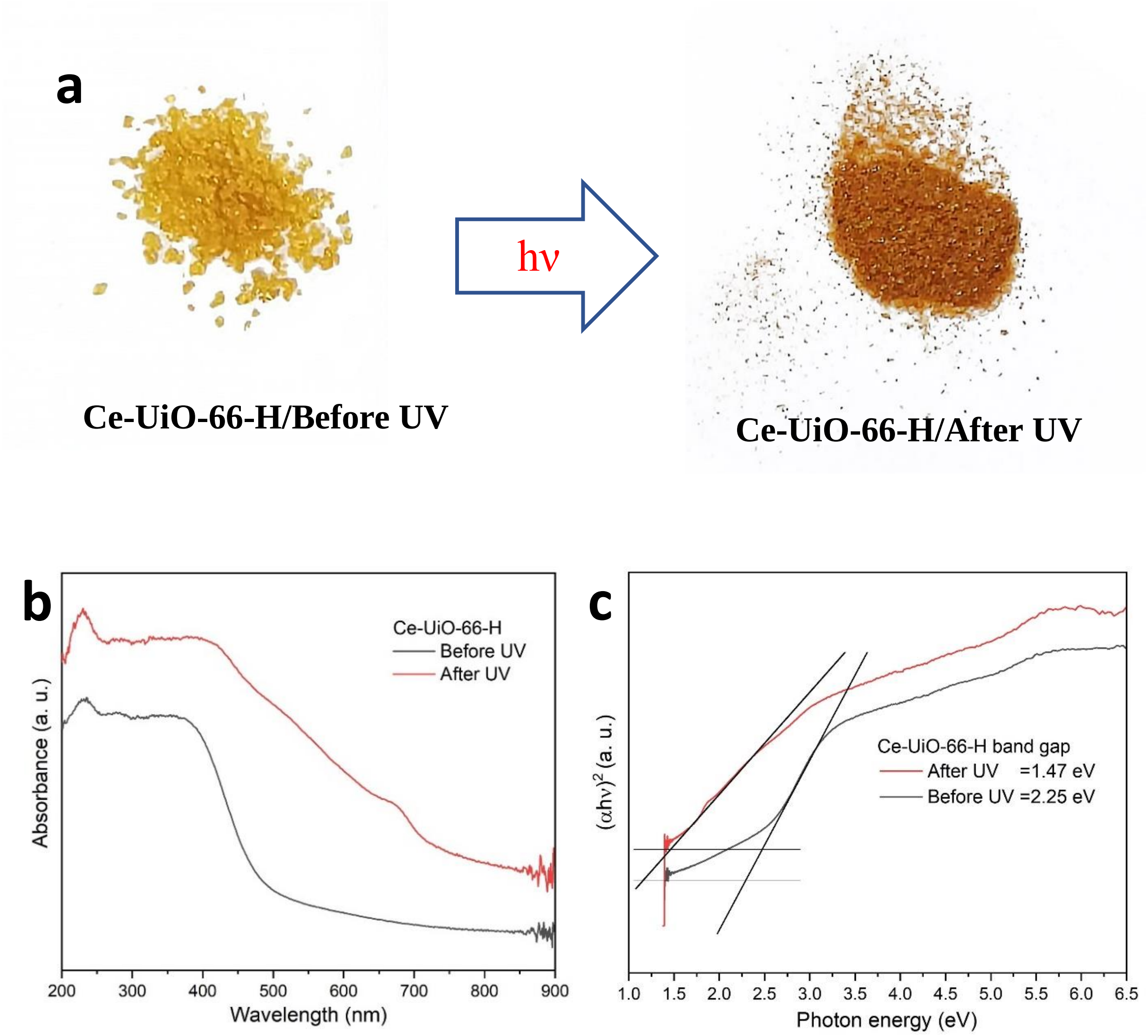

Figure S7: a) The colour change in Ce-UiO-66-H before UV and after UV irradiation, b) DR/UV-Vis of Ce-UiO-66-H before and after UV irradiation, c) the band gap of the sample before and after UV irradiation calculated by Tauc plots.

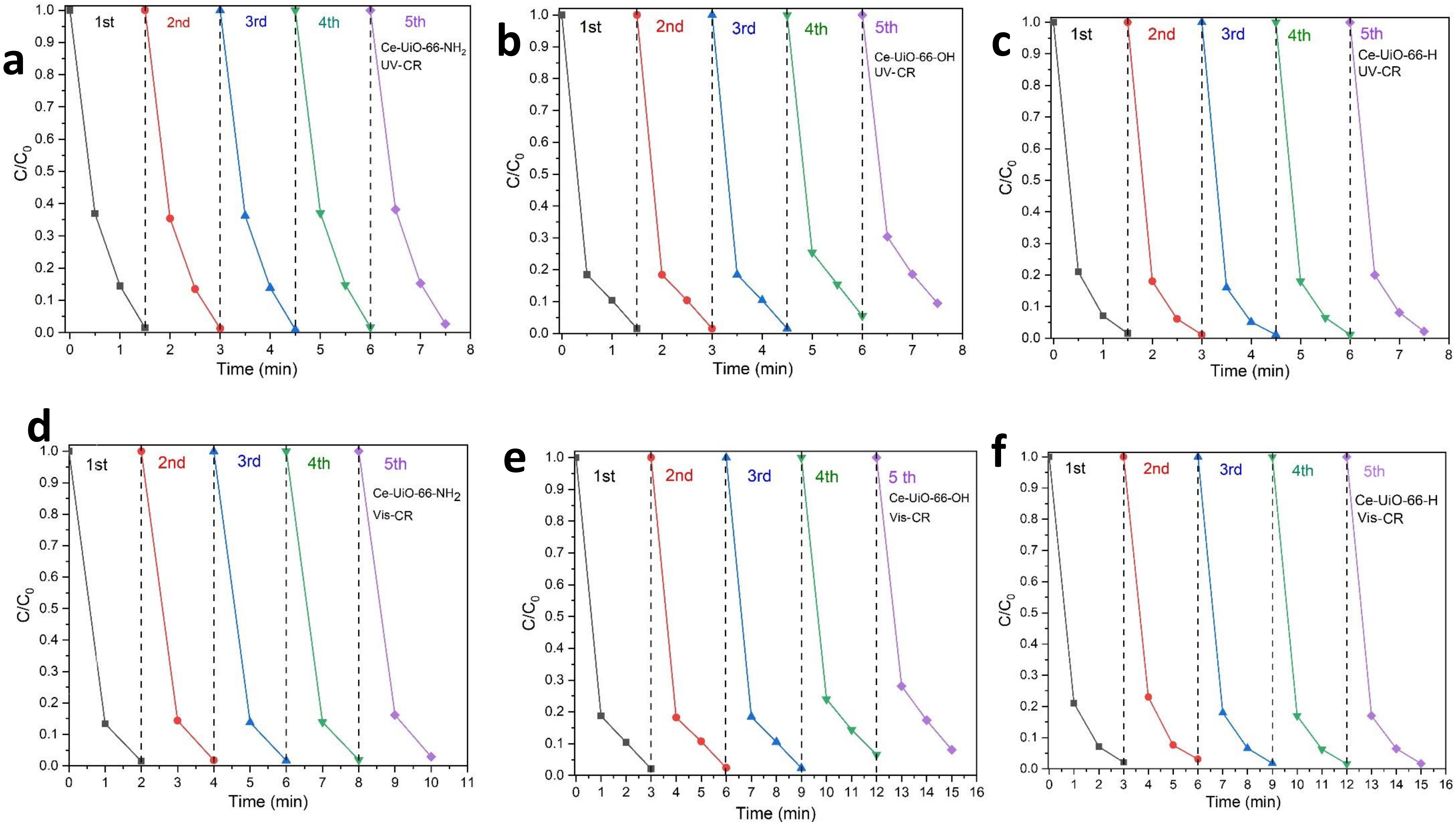
a
C/C$_0$
Time (min)
1st
2nd
3rd
4th
5th
Ce-UiO-66-NH$_2$
UV-CR
0.0
0.1
0.2
0.3
0.4
0.5
0.6
0.7
0.8
0.9
1.0
0
1
2
3
4
5
6
7
8
b
C/C$_0$
Time (min)
1st
2nd
3rd
4th
5th
Ce-UiO-66-OH
UV-CR
c
C/C$_0$
Time (min)
1st
2nd
3rd
4th
5th
Ce-UiO-66-H
UV-CR
d
C/C$_0$
Time (min)
1st
2nd
3rd
4th
5th
Ce-UiO-66-NH$_2$
Vis-CR
0
1
2
3
4
5
6
7
8
9
10
11
e
C/C$_0$
Time (min)
1st
2nd
3rd
4th
5 th
Ce-UiO-66-OH
Vis-CR
0
1
2
3
4
5
6
7
8
9
10
11
12
13
14
15
16
f
C/C$_0$
Time (min)
1st
2nd
3rd
4th
5th
Ce-UiO-66-H
Vis-CR

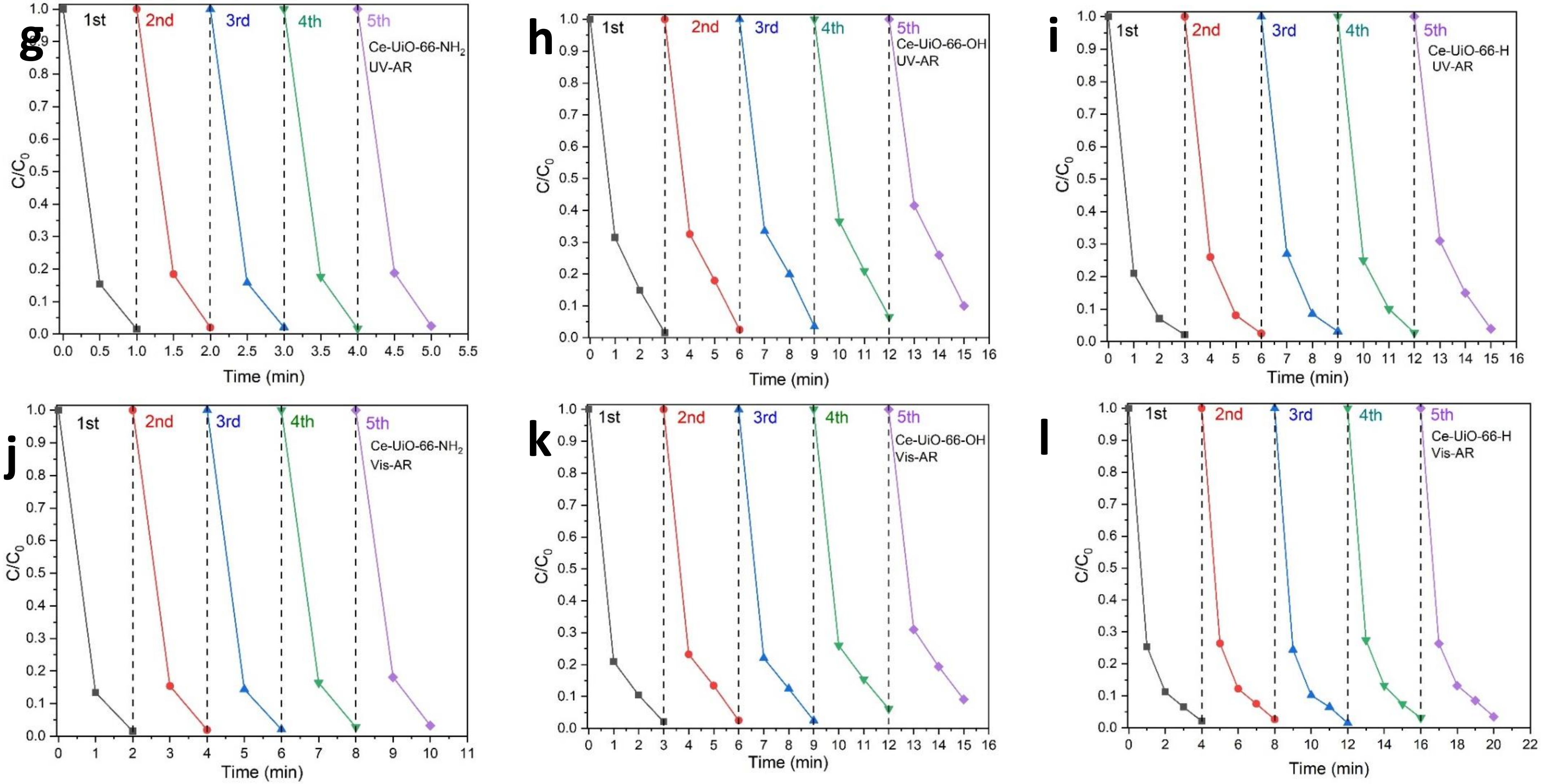

Figure S8: Recyclability measurements of Ce-UiO-66-X (X=NH$_2$, OH, H) over 5 cycles in AR and CR, under UV and visible light irradiation at room temperature, a) Ce-UiO-66-NH$_2$ in CR under UV light, b) Ce-UiO-66-OH in CR under UV light, c) Ce-UiO-66-H in CR uner UV light, d) Ce-UiO-66-NH$_2$ in CR under visible light, e) Ce-UiO-66-OH in CR under visible light, f) Ce-UiO-66-H in CR under visible light, g) Ce-UiO-66-NH$_2$ in AR under UV light, h) UiO-66-OH in AR under UV light, i) Ce-UiO-66-H in AR under UV light, j) Ce-UiO-66 in AR under visible light, k) Ce-UiO-66-OH in AR under visible light, l) Ce-UiO-66-H in AR under visible light.

Table S3: Photocatalysis properties of MOFs reported in previous studies showing the method of synthesis, band gap, dyes, source of light, time, degradation rates, recyclability, and stability. The missing entries are not reported in the original literature.

Material	Method of synthesis/time (h)	Band gap (eV)	Dye(s)	Irradiation	Time (min)	Degradation rate (%)	Recyclability (runs)	Stability (h)	Ref
Cu(II)-pyrazole MOF	Solvothermal/72	2.031	MB-MO	UV	120	90	-	1.5	[2]
g-C_3N_4/MIL-125	Solvothermal/48	3.1	RhB	Visible	60	100	5	5	[3]
g-C_3N_4/MIL-53(Al)	Stirring/12	2.64	RhB	Visible	75	100	5	6.2	[4]
AgI/UiO-66(Zr)	-	2.83	RhB	Visible	60	100	5	5	[5]
Ag/AgCl/ZIF-8	Stirring/13	0.5	RhB	Sun	16	100	6	1.4	[6]
TiO_2	Microwave	2.05	RhB	Visible	300	60	-	-	[7]
g-C_3N_4/UiO-66 (Zr)	Solvothermal/24	3.74	RhB	Visible	180	100	4	12	[8]
TiO_2/GO (7/11)	Stirring/12	-	MB	Visible	20	90	3	1	[9]
UiO-66(Ce/Ti)	Reflux/3	2.84	TC	Visible	60	80	3	3	[10]
NNU-15(Ce)	Solvothermal/72	2.11	RhB	Visible	12	95	5	1	[11]
UiO-66	Solvothermal/24	3.91	RhB-CR	Vis	120	10	-	-	[12]
UiO-66(NH_2)	Solvothermal/24	2.83	RhB-CR	Vis	120	10	-	-	[12]
UiO-66$(OH)_2$	Solvothermal/24	2.69	RhB-CR	Vis	120	70	-	-	[12]
UiO-66$(SH)_2$	Solvothermal/24	2.75	RhB-CR	Vis	120	70	-	-	[12]
UiO-66(Br)	Solvothermal/24	3.69	RhB-CR	Vis	120	70	-	-	[12]
UiO-66(NH_2)	Solvothermal/24	2.90	Cr(IV)	Vis	120	100	20	38	[13]
NH_2-MIL-101(Fe)	Solvothermal/48	1.32	RhB	Vis	180	100	4	16	[14]
UiO-66(NH_2)	Solvothermal/24	2.83	MB	UV	120	97.7	-	-	[15]
BiOBr@UiO-66	Solvothermal/24	2.9	RhB	Vis	30	100	6	-	[16]

TC= tetracycline

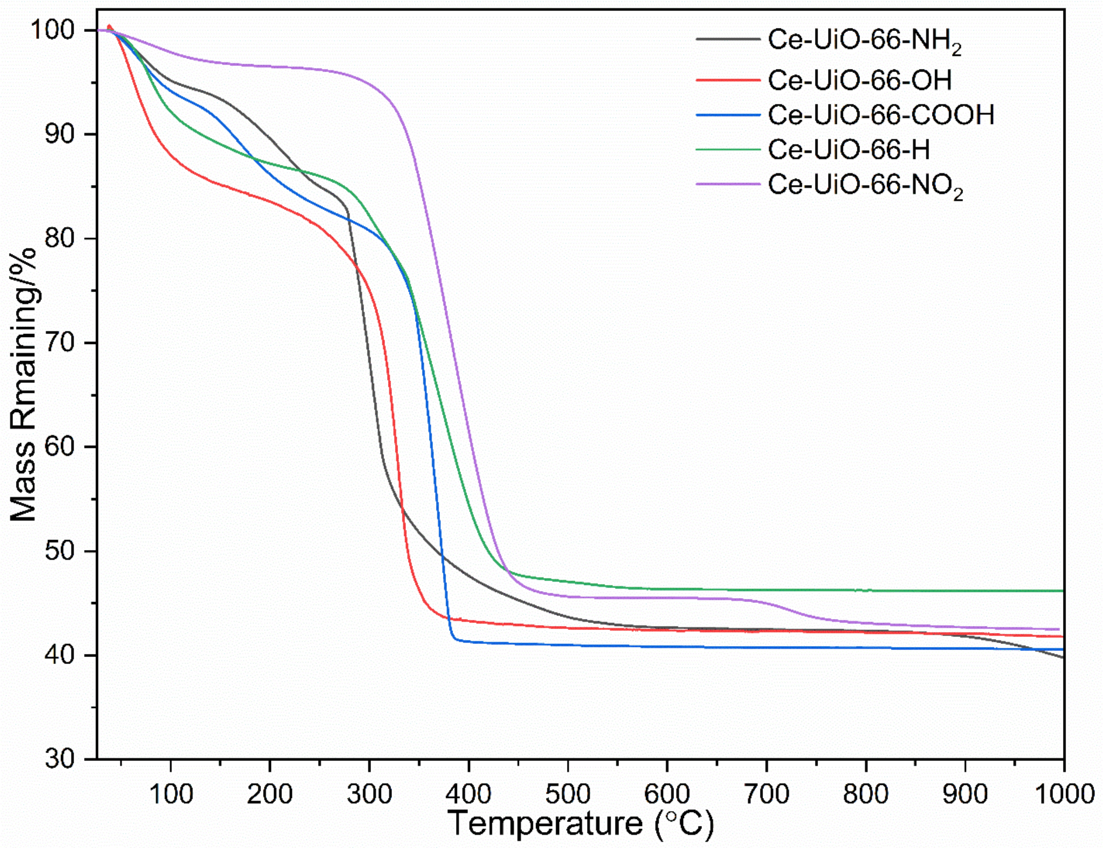

Figure S9: Thermogravimetric analysis of Ce-UiO-66-X materials measured in air (heating rate 10 °C min^{-1}*)*

The chemical formula of the materials can be written as:

$Ce_6O_4(OH)_4(BDC\text{-}X)_{6\text{-}N}(OH)_{2N}(H_2O)_{2N}\cdot(solvent)_x$

Where solvent = DMF and water, and the ligand defects are charge balanced by hydroxide ions with additional water to complete the coordination sphere of Ce.

This can be written as:

$Ce_6O_4(OH)_4(BDC\text{-}X)_n(OH)_{2(n-6)}(H_2O)_{2(n-6)}\cdot(solvent)_x$

The UiO-66 mass loss to ~ 350°C is the elimination of the water and other solvent trapped in the pores and dehydroxylation of the clusters.

$Ce_6O_4(OH)_4(BDC\text{-}X)_n(OH)_{2(n-6)}(H_2O)_{2(n-6)}\cdot(solvent)_x \rightarrow Ce_6O_6(BDC\text{-}X)_n(O)_{6\text{-}n}$ + solvent + H_2O

This assumes the charge is balanced by some retained oxide taking the place of linker defects, and the other oxygen sites are vacant. Upon continued heating the remaining hydroxide and the ligand is lost to yield CeO_2 above 500 °C. Note that continued heating gives further loss of oxygen to yield CeO_{2-x}.

Thus, irrespective of the amount of solvent present initially the unknown value *n* can be determined from the mass losses at each step: the results are shown in Table 4 of the main text.

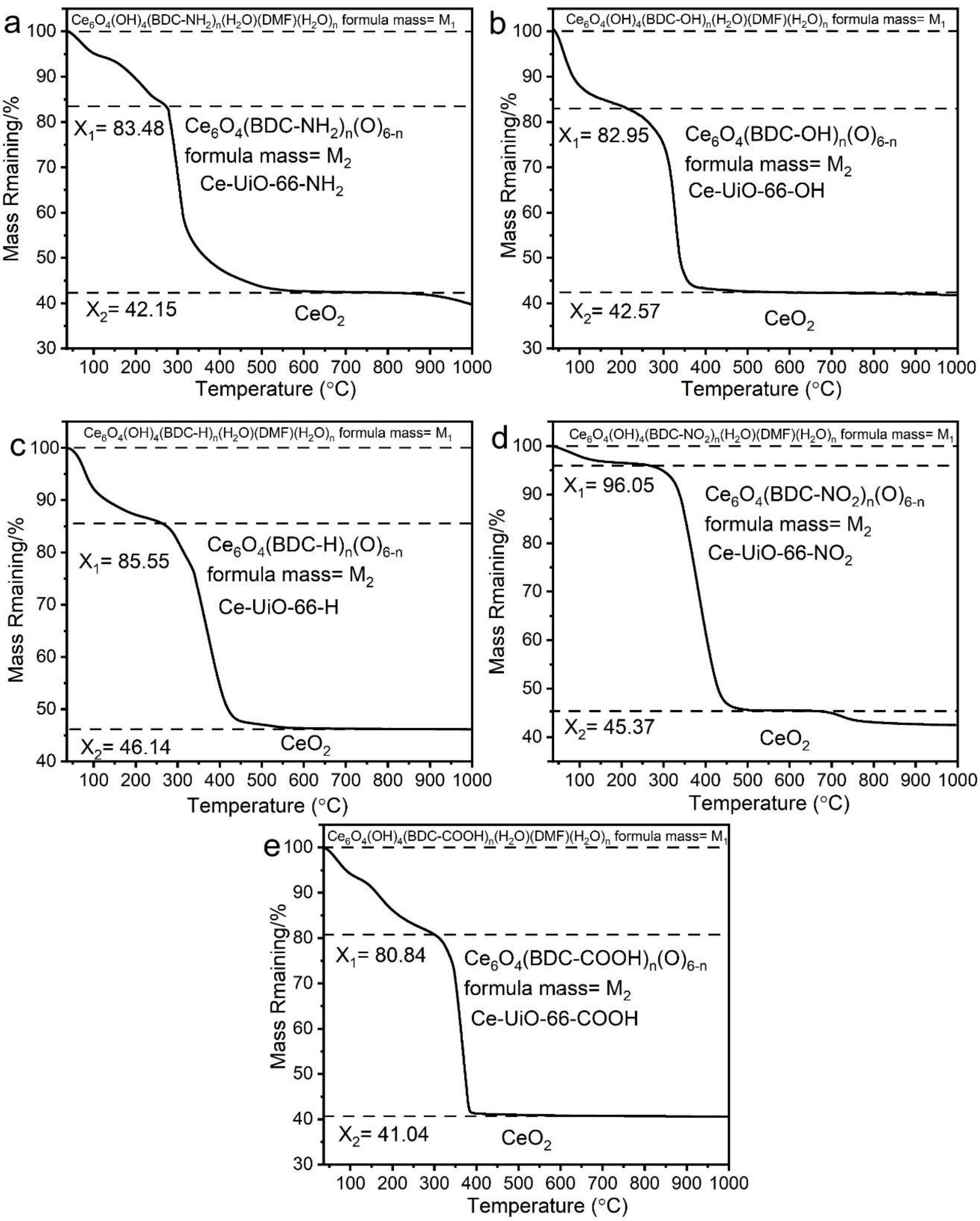

Figure S10: Thermogravimetric analysis of Ce-UiO-66-X materials measured in air (heating rate 10 °C min^{-1}) with observed % mass losses indicated. The results of analysis are shown in Table 4 of the main paper.

TOC analysis was performed using a Shimadzu analyzer. The clear solution remaining after photocatalytic degradation of 15 mg of Congo Red in 200 mL water using 25 mg of the material Ce-UiO-66-NH_2 was analysed.

The initial carbon content of the Congo Red solution was equivalent to 8.27 mg in 200 mL (CR contains 55 % carbon by mass).

160 mL of the product solution was diluted with 800 mL deionised water for TOC analysis, and this gave a result of 1.66 ppm.

The maximum carbon content possible in the diluted solution is (160/200)*8.27 mg in 960 mL = 6.89 mg L^{-1} = 6.89 ppm.

Therefore around 25 % of the original carbon is present in solution as soluble carbon species. The remainder may have been lost as CO_2, or have been adsorbed by the MOF.

References

1. M. Rubio-Martinez, M. P. Batten, A. Polyzos, K.-C. Carey, J. I. Mardel, K.-S. Lim and M. R. Hill, *Sci. Rep.*, 2014, **4**, 5443.
2. S. Bala, S. Bhattacharya, A. Goswami, A. Adhikary, S. Konar and R. Mondal, *Cryst. Growth. Des.*, 2014, **14**, 6391-6398.
3. H. Wang, X. Yuan, Y. Wu, G. Zeng, X. Chen, L. Leng and H. Li, *Appl. Catal. B.*, 2015, **174-175**, 445-454.
4. D. Guo, R. Wen, M. Liu, H. Guo, J. Chen and W. Weng, *Appl. Organomet. Chem.*, 2015, **29**, 690-697.
5. Z. Sha, J. Sun, H. S. O. Chan, S. Jaenicke and J. Wu, *Chem. Plus. Chem.*, 2015, **80**, 1321-1328.
6. S.-T. Gao, W.-H. Liu, N.-Z. Shang, C. Feng, Q.-H. Wu, Z. Wang and C. Wang, *RSC. Adv.*, 2014, **4**, 61736-61742.
7. K. Kato, Y. Xin and T. Shirai, *Sci. Rep.*, 2019, **9**, 4900.
8. X. Zhang, Y. Yang, W. Huang, Y. Yang, Y. Wang, C. He, N. Liu, M. Wu and L. Tang, *Mater. Res. Bull.*, 2018, **99**, 349-358.
9. Y. Li, B. Lin, L. Ge, H. Guo, X. Chen and M. Lu, *Sci. Rep.*, 2016, **6**, 28803.
10. Y. Zhang, H. Chen, Y. Pan, X. Zeng, X. Jiang, Z. Long and X. Hou, *Chem. Commun.*, 2019, **55**, 13959-13962.
11. Q. Xia, X. Yu, H. Zhao, S. Wang, H. Wang, Z. Guo and H. Xing, *Cryst. Growth. Des.*, 2017, **17**, 4189-4195.
12. X. Mu, J. Jiang, F. Chao, Y. Lou and J. Chen, *Dalton. Trans.*, 2018, **47**, 1895-1902.
13. X.-D. Du, X.-H. Yi, P. Wang, W. Zheng, J. Deng and C.-C. Wang, *Chem. Eng. J.*, 2019, **356**, 393-399.
14. Q. Wang, Q. Gao, A. M. Al-Enizi, A. Nafady and S. Ma, *Inorg. Chem. Front.*, 2020, **7**, 300-339.
15. Q. Chen, Q. He, M. Lv, Y. Xu, H. Yang, X. Liu and F. Wei, *Appl. Surf. Sci.*, 2015, **327**, 77-85.
16. H. Tian, Y. Gu, H. Zhou, Y. Huang, Y. Fang, R. Li and C. Tang, *Mater. Sci. Eng. B.* , 2021, **271**, 115297.